

# **A $\beta$ immunotherapy reduces amyloid plaques and astroglial reaction in aged domestic dogs**

Maria Neus Bosch, Marco Pugliese, Carmen Andrade, Javier Gimeno-Bayón, Nicole Mahy and Manuel J Rodríguez

Unitat de Bioquímica i Biologia Molecular, Facultat de Medicina, Institut d'Investigacions Biomèdiques August Pi i Sunyer (IDIBAPS), Universitat de Barcelona and Centro de Investigación Biomédica en Red sobre Enfermedades Neurodegenerativas (CIBERNED), c/Casanova 143, 08036, Barcelona, Spain.

\* Author for correspondence: Dr. Manuel J. Rodríguez

Unitat de Bioquímica i Biologia Molecular

Facultat de Medicina, UB

C/ Casanova 143

E-08036 Barcelona, SPAIN

Phone: (+34) 93 402 0586

Fax: (+34) 93 403 5882

E-mail: marodriguez@ub.edu

KEY WORDS: Amyloid  $\beta$ , Alzheimer's disease, Immunotherapy, Cognitive dysfunction syndrome, astroglia, microglia

GRANT INFORMATION: This work was supported by grant IPT-2012-0614-010000 from the Ministerio de Economía y Competitividad and grant 2009SGR1380 from the Generalitat de Catalunya, Spain

## **ABSTRACT**

**Background:** Alzheimer's disease (AD) is characterized by the dynamic accumulation of extracellular amyloid deposits from the interplay between amyloid- $\beta$  (A $\beta$ ) plaques, reactive astrocytes and activated microglia. Several immunotherapies against A $\beta$  have been shown to reduce amyloid neuropathology. However, the role of the associated glia in the recovery process requires clarification. Previously, we described the safety and effectiveness in aged domestic canine with cognitive dysfunction syndrome of a new active vaccine candidate for the treatment of AD in humans.

**Objective:** The aim of this article is to gain a better understand of how immunotherapy modifies the amyloid burden and its effects on astroglial and microglial reactivity in immunized dogs.

**Methods:** In order to achieve this, we compared and quantified amyloid plaques and astroglial and microglial reactions in the frontal cortex of unimmunized and immunized aged domestic dogs.

**Results:** We found amyloid plaques from immunized dogs to be smaller and more compact than those from unimmunized dogs. In these new plaques, the associated astrocytes were closer and less immunoreactive to S100B. We also found no modification in the microglial reaction associated with immunization.

**Conclusion:** The anti-A $\beta$  immunotherapy developed in our laboratory modifies the equilibrium between soluble and insoluble A $\beta$  in aged dogs in close correlation with S100B-negative astrocytosis and microglial reaction.

## INTRODUCTION

Alzheimer's disease (AD) is characterized by the accumulation of intracellular neurofibrillary tangles and different forms of extracellular amyloid- $\beta$  ( $A\beta$ ) (monomers, oligomers, fibrils and plaques) resulting from amyloid precursor protein (APP) processing [1,2]. These soluble oligomers, fibrils and amyloid plaques are usually in equilibrium between brain tissue, cerebrospinal fluid (CSF) and blood compartments. However, the imbalance between  $A\beta$  production and clearance in AD leads to the accumulation of these amyloid components [3]. Also, changes in the biochemical composition of  $A\beta$  aggregates oligomers, protofibrils, and fibrils are specifically associated with symptomatic occurrence of AD [4]. Thus, the imbalance between soluble  $A\beta$  production and clearance modifies the amyloid plaque features [5] and the glial response [6]. The resulting abundance of amyloid deposits is an interplay between plaques of different biochemical composition, reactive astrocytes and activated microglia [6–8].

One of the animals considered to be a good model for research into mild cognitive impairment and AD is the aged domestic dog (over eight years old) with cognitive dysfunction syndrome (CDS) [9–12]. Since this animal spontaneously develops geriatric behavioral changes related to several markers of sporadic AD (soluble  $A\beta$ ,  $A\beta$  diffuse plaques and brain atrophy), early AD physiopathology mechanisms and new therapeutic targets for innovative therapies can be researched through studies performed using CDS dogs [12–14]. Beginning around age eight, the formation and maturation of diffuse  $A\beta$  deposits are observed by immunostaining in all layers of canine cortical grey matter in a characteristic four-stage distribution that correlates with the CDS severity degree and astroglial reaction [15–18]. Despite the human studies that suggest an association between amyloid plaque stages and the degree of microglial activation [20,21], there is still controversy surrounding the activation of microglia by diffuse plaques. The contradictory results are probably due to differences

in the antibodies and lectins used for detection [6,22].

Astrocyte overexpression of the beta-subunit of S100 protein (S100B) plays a role in the pathogenesis and progression of AD and other neurodegenerative diseases through autocrine and paracrine effects on astrocytes, neurons and microglia [23]. In AD, most of these S100B-positive astrocytes are closely associated with both diffuse and neuritic plaques [24], and their distribution throughout the brain regions mirrors the known distribution patterns for A $\beta$  deposits [25]. In CDS dogs, the astrocyte proliferation around diffuse plaques was found to be S100B negative, which together with the absence of neuritic plaques in the dog brain would suggest an important pathogenic role for S100B in the genesis and evolution of AD plaques [20,24].

Many anti-A $\beta$  immunotherapies targeting soluble and/or insoluble A $\beta$  [26,27] have been tested as ways of preventing or treating AD in animals and humans [28–32]. Due to the initial severe adverse effects observed in humans [33,34], further studies focused on the design of effective and safe immunotherapy [35,36]. One of these immunotherapies, based on a mixture of fibrillar A $\beta$  components, has been developed in our laboratory with great effectiveness and complete safety in domestic dogs with CDS [37]. In that study, the vaccine led to a very rapid cognitive improvement in all treated animals, with no side effects.

To gain a better understanding of how immunotherapy modifies the amyloid burden and its effects on astroglial and microglial reactivity, we quantified amyloid plaques and astroglial and microglial reactions in brain samples from unimmunized and immunized male and female domestic dogs of different ages and breeds and with different cognitive deficits. To avoid the controversy surrounding canine microglia quantification with antibodies and lectins, we estimated the microglial reaction by *in vitro* autoradiography of [ $^3$ H]PK11195 binding to the peripheral benzodiazepine receptor (PBR) [38–41].

## **MATERIALS AND METHODS**

### **Vaccine**

The fibrillar A $\beta$  vaccine was initially prepared with 100  $\mu$ g of A $\beta$ <sub>40</sub> combined with the A $\beta$ <sub>x-40</sub> peptide KLH conjugated. A $\beta$ <sub>40</sub> and A $\beta$ <sub>x-40</sub> peptides were initially dissolved with dimethyl sulfoxide (DMSO) (1mg/ml), aliquoted and stored at -20°C. Once thawed, each A $\beta$  peptide was mixed with 1 mg of alum hydroxide suspension (Sigma, Spain). After overnight (ON) incubation at 4°C, a saline solution was added up to a volume of 1.5 ml prior to the subcutaneous (SC) immunization of the dogs.

### **Animals**

Twenty-three male and female domestic dogs of different ages and breeds and with different cognitive deficits were included in the study (Table 1). All dogs were previously classified as non-demented dogs (n=12) or CDS dogs (n=11), depending on the score obtained using a validated cognitive test of nine items adapted from the mini-mental state examination (MMSE) and the Diagnostic and Statistical Manual of Mental Disorders (DSM IV) for AD [10,12]. Five of these 23 dogs had been included in a previous immunization study performed by our group [37] in which they received six SC injections of the fibrillar A $\beta$  vaccine over a period of 51 days and were sacrificed at the end of the immunization study after blood extraction (Fig.1, Table 1). One of the immunized dogs presented CDS symptoms at the beginning of the immunization period.

All animals were treated according to European legislation on animal handling and experimentation (86/609/EU). Procedures were approved by the University of Barcelona Ethics Committee, Barcelona, Spain. All efforts were made to minimize animal suffering and to use no more than the number of animals required to obtain reliable scientific data.

### **Brain tissue preparation**

Animals were euthanized with an IV overdose of sodium thiopental (75 mg/kg) (Thiobarbital, Braun Medical S.A., Spain) and tissue preparation was adapted from human brain bank methods [42]. In all cases, donation was formally approved by the owner and euthanasia justified for medical reasons, none of which were related to immunotherapy. The dog brains were removed immediately following death. Both hemispheres were separated and cut into 1-cm thick coronal sections. One hemisphere was frozen in powdered dry ice and stored at  $-80^{\circ}\text{C}$ . The other hemisphere was fixed by immersion in cold 4% formaldehyde (PFA) diluted in 10 mM phosphate buffer (PB, pH 7.4) for four days. After three days of cryoprotection, they were frozen on powdered dry ice and kept at  $-40^{\circ}\text{C}$  until use. Some liver and spleen samples were also collected as tissue control for histological procedures.

### **Anti-A $\beta_{40}$ IgGs purification**

pH gradient elution by immunoaffinity column was used for the anti-A $\beta_{40}$  purification. For this, Sepharose powder (Pharmacia, Barcelona, Spain) activated with cyanogen bromide and coupled to the A $\beta_{40}$  peptide (40 amino acid length) was placed into a chromatography column (Bio-Rad, CA, USA). After being washed with 10 ml of 100 mM cold phosphate buffer saline (PBS, pH 7.4), 1 ml dog serum was loaded into the column three times. After being washed with 10 ml cold PBS, anti-A $\beta_{40}$  Igs were eluted by pH gradient using firstly 100 mM glycine, pH 2.5 and secondly 100 mM glycine + 4M urea, pH 2.5. 200  $\mu\text{l}$  of antibody fractions were collected in Eppendorf tubes containing 1M Tris, pH 8. Anti-A $\beta_{40}$  IgGs were detected in each Eppendorf tube using a dot blot method. Briefly, antibody samples were loaded on a PVDF membrane (Bio-Rad, Madrid, Spain) and incubated for 1 h with biotinylated anti-dog IgG (LifeSpan Biosciences, Derio, Spain). Detection was carried out by incubation in 20 mM Tris-

HCl,- 137 mM NaCl (TBS, pH 7.4) containing 0.03% 3-3' diaminobenzidine (DAB) and 0.006% H<sub>2</sub>O<sub>2</sub>. Finally, purified antibodies were dialyzed, concentrated to half of the volume in 50 mM Tris-HCl, pH 7.4 and stored at -20°C until use.

### **Immunohistochemistry**

To detect amyloid plaques and immunoreactive astrocytes on dog sections, immunohistochemistry with specific antibodies against A $\beta$  peptide (Dako, Glostrup, Denmark), S100B (Dako, Glostrup, Denmark) and Glial Fibrillary Acidic Protein (GFAP) (Dako, Glostrup, Denmark) was carried out on 12- $\mu$ m thick serial sections obtained from the PFA-fixed frontal cortex. To detect amyloid plaques on human sections, purified dog anti-A $\beta$ <sub>40</sub> antibodies from immunized CDS dogs or commercial mouse anti-A $\beta$  antibodies (Dako, Glostrup, Denmark) were used for the immunohistochemistry. For comparisons, immunohistochemistry was carried out in 5- $\mu$ m thick sections from frontal cortex samples of AD human brain. Paraffined fixed brain tissues from AD patients at stage II and VI according to the Braak & Braak scale [43] were obtained from the Neurological Tissue Bank of the Universitat de Barcelona (Barcelona, Spain).

Some sections were stained with Perl's Prussian blue counterstained with neutral red to identify hemosiderin deposits resulting from putative microhemorrhages [44]. For immunohistochemistry, slices were deparaffined or defrosted and pre-treated in formic acid for 2 min. After endogenous peroxidase inhibition for 30 min, the slices were incubated with PBS 100mM, pH 7.4, containing 0.5% triton-X100-5% normal goat serum (NGS) - 5% Bovine Serum Albumin (BSA) as a blocking agent for 2 h at RT. Purified primary antibodies or commercial mouse anti-A $\beta$  antibodies were diluted (1/100) with immunobuffer (PBS- 5% triton-X100-1% NGS - 1% BSA) and incubated ON at 4°C. After being washed with PBS, the samples were incubated with 1/4000 diluted biotinylated anti-dog IgG or 1/100 diluted biotinylated anti-mouse IgG for 2 h. After washing, the slices were incubated for 1 h with ExtrAvidin (1/250) and developed with 0.03% DAB 0.006% H<sub>2</sub>O<sub>2</sub> in PBS. Some sections were also incubated with anti-

CD3 (1:300; AbD Serotec, Oxford, UK) followed by biotinylated anti-mouse IgG, for immunodetection of infiltrated lymphocytes.

Double detection of amyloid plaques / astrocytes was performed by sequential immunohistochemistry. Amyloid plaques were first stained in black with anti-A $\beta$  antibody (diluted 1/100) as described above, and developed by adding NiCl to the developing solution to stain astrocytes brown on the same slices. Sections were incubated with 1/250 diluted rabbit anti-GFAP antibody or with diluted 1/500 rabbit anti-S100B antibody detected with biotinylated anti-rabbit IgG (1/500) and developed with 0.03% DAB-0.006% H<sub>2</sub>O<sub>2</sub> in PBS. To reduce the variability due to immunolabeling procedures, for each specific antibody all slices were processed at the same time, using the same antibody solutions, and incubation / reaction and developing times.

Plaques and astrocytes were visualized by optical microscopy (Olympus America Inc., NY, USA) and micrographs were taken at 5x and 40x following the same image thresholding and acquisition protocol. The number and reactivity of plaques and GFAP-S100B immunoreactive astrocytes were quantified in dog samples, as previously described [20] For this, five semi-randomized micrographs were taken and analyzed (Axio-Vision, Carl Zeiss, Germany) in three conditions: 1) to measure the number, area and grey color intensity of plaques, we obtained photomicrographs, at a magnification of 5x, of the whole frontal cortex area; 2) to measure the number and grey color intensity of immunoreactive astrocytes, we obtained photomicrographs, at a magnification of 40x, from the frontal cortex; and 3) to estimate the number and grey color intensity of immunoreactive astrocytes found within 200  $\mu$ m of the most external part of the plaque, we obtained photomicrographs, at a magnification of 10x, from the same five frontal cortex plaques. To improve data reliability, GFAP and S100B immunohistochemistry were performed on serial slices and the same semi-randomized areas in white matter, and the same semi-randomized plaques were used for all parameters analyzed.

### **Thioflavin-T-positive (ThT+) detection of amyloid plaques by purified anti-A $\beta$ <sub>40</sub> IgGs**

ThT+ detection of diffuse amyloid plaques by purified anti-A $\beta$ <sub>40</sub> IgGs was carried out on 5- $\mu$ m thick slices from the frontal cortex of AD patients at stage II according to the Braak & Braak scale [45]. First, A $\beta$  plaques were detected following the immunohistochemistry procedure and using purified dog anti-A $\beta$ <sub>40</sub> from immunized CDS dogs or commercial mouse anti-A $\beta$  antibodies, as described above. The slices were then dried in the dark at 4°C ON, rehydrated and immersed in a solution of 0.05% ThT-HCl 0.1M. Afterwards, they were incubated with 1% acetic acid for 20 min, washed and mounted with Prolong Antifade reagent (Sigma Aldrich, MO, USA). Plaques were visualized by fluorescence microscopy (Carl Zeiss, Germany) and photomicrographs were taken at a magnification of 20x.

### ***In vitro* autoradiography binding of the [<sup>3</sup>H]PK11195 to the peripheral benzodiazepine receptor (PBR)**

Autoradiographic labeling of PBR, a specific marker of microglia, was performed with [<sup>3</sup>H]PK11195 (NEN, Boston, MA, USA) on 5- $\mu$ m thick serial sections of frozen entorhinal cortex, as described previously [38-40]. Sections were incubated in an ice-cold 50 mM Tris-HCl solution (pH 7.7) containing 1 nM [<sup>3</sup>H] PK11195 for 2 h at RT, followed by two rinses in 4°C Tris-HCl buffer for 5 min. Non-specific binding was determined in the presence of 1 mM unlabeled PK11195. After rinsing in water, sections were dried under a stream of cold air and apposed to Amersham Hyperfilm (Amersham, Bucks, UK) for two weeks. Films were developed and analyzed densitometrically after calibration with grey scales (3H-microscales; Amersham) using the Image-Pro Plus program (MD, USA). The average brain protein content was 8%. For each brain, four sections were processed for total binding and two others for non-specific binding. The values obtained for each brain after non-specific binding subtraction were averaged and used for statistical comparisons.

### **Statistical analysis.**

Kurtosis and skewness were calculated to verify the normal distribution of data. One-way ANOVA was performed to compare the plaque, astroglia and microglia parameters between the treatment and plaque stage, followed by Fisher's LSD and Bonferroni post-hoc tests. To quantify the association between two variables, a Pearson correlation was performed. When normality was not achieved, the values of all groups were compared using non-parametric analysis. In these cases, the Kruskal-Wallis test (KW) followed by the Mann-Whitney test (MW) were used to compare dependent variable groups, and the Spearman correlation was used to quantify the association between two variables. In all cases,  $p < 0.05$  was considered as significant. Results are expressed as a mean  $\pm$  SEM. All analyses were performed with the programs SPSS 17 (IBM Spain, Madrid, Spain) and STATGRAPHICS (STSC Inc., Rockville, MD, USA).

## RESULTS

### Increased cortical microglial reaction in CDS dogs

Initially, astroglial and microglial reactivity was compared between unimmunized control (n = 8) and CDS (n = 10) dogs. To this end, four parameters (number of S100B; number of GFAP immunoreactive (IR) astrocytes; grey color intensity of S100B-positive astrocyte cytoplasm; and binding of [<sup>3</sup>H]PK11195) were measured in the cortex of both groups. In CDS dogs, the number of S100B-IR and GFAP-IR both showed a non-significant tendency to increase (Fig. 2A, C), but we found no differences in the intensity of S100B labeling (Fig. 2B).

To study the microglial reaction, [<sup>3</sup>H]PK11195 autoradiography was performed. [<sup>3</sup>H]PK11195-specific binding showed low levels (between 551 and 1068 fmol/mg prot) in the cortex of control dogs, with the lowest values in the internal layers of this area (Fig. 4H). Non-specific binding was homogeneous and very low, representing less than 10% of the total binding. In the cortex of CDS dogs, [<sup>3</sup>H]PK11195-specific binding was 29.40% higher when compared with controls (p=0.034). This increase in specific labeling was homogeneously distributed in the tissue, and no cluster-associated labeling was observed in any layer of the prefrontal cortex (Fig. 5H)

When data from immunized dogs were included in the study, the intensity of S100B-IR showed a non-significant tendency to decrease in all animals. However, no differences were found in the number of S100B-IR or GFAP-IR cells or in the [<sup>3</sup>H]PK11195-specific binding (Fig. 2A-D).

### Anti-A $\beta_{40}$ IgGs from immunized dogs recognize diffuse plaques

Previously, we showed that this vaccine in dogs generates anti-A $\beta_{40}$  IgGs that cross the blood-brain barrier (BBB) and bind to human diffuse plaques [37]. To determine whether or not they bind similarly to human neuritic, diffuse and fibrillar amyloid plaques in AD stage II and VI, serum from dogs was taken on day 51 of the

immunization period. Purified anti-A $\beta_{40}$  IgGs presented stronger immunoreactivity to diffuse plaques than neuritic ones. These antibodies were not IR to ThT+ plaques or blood vessels (Fig. 3). A similar study performed with commercial anti-A $\beta_{40}$  IgGs showed an increased IR to neuritic plaques (Fig. 3).

### **Immunization reduces the size of amyloid plaques and increases their compaction**

Prussian blue histochemistry revealed no hemosiderin deposits (Fig. 4A-C) in the prefrontal cortex of none of the five immunized dogs, including the one presenting CDS. Also, we found no specific CD3-positive staining by immunohistochemistry in none of the samples (Fig. 4D-F).

To determine whether or not the immunization process modifies them, we characterized amyloid plaques by immunohistochemistry in three immunized dogs and nine control aged animals (older than eight, since young animal brains do not form any plaques). We identified two groups of non-immunized dogs, according to the size, density and cortical-layer distribution of amyloid plaques, as previously described [12]; five dogs presented diffuse amyloid plaques (stage I-II) that had a “cloud-like” aspect, covered a large area, were poorly compacted, and were located in layers V-VI of the prefrontal cortex (Fig. 5A-C). Four dogs presented more compact amyloid plaques (stage III-IV) that were smaller in size, more aggregated and located in layers II-III or throughout all layers of the prefrontal cortex (Fig. 5A-C). The three immunized dogs presented different specific plaques, which were the smallest in size and had a more dense aspect than the stage I-II and stage III-IV plaques ( $p=0.036$  and  $p=0.033$  respectively; Fig. 5A-C). The plaque distribution in these animals was similar to that of the stage III-IV plaques, since they were located in layers II-III or throughout all layers of the frontal cortex.

### **Immunization decreases immunoreactivity to S100B**

A comparison of the astroglial reaction of dogs classified by amyloid plaque morphology showed no difference in the number of S100B-IR and GFAP-IR astrocytes (Fig. 5D,F). However, immunized dogs presented a lower intensity of S100B-positive astrocyte cytoplasm than the other groups ( $p=0.016$ ; Fig. 5E). Moreover, both GFAP-IR and S100B-IR astrocytes in the prefrontal cortex of immunized dogs presented a lower number of cell processes than astrocytes in the prefrontal cortex of non-immunized animals amyloid plaques (Fig. 6A,B).

We also quantified microglial activation by [ $^3\text{H}$ ]PK11195 autoradiography. In all animals presenting amyloid plaques, the levels of [ $^3\text{H}$ ]PK11195-specific binding sites in the cortex showed a marked increase when compared to young controls (mean 28.95% increase;  $p=0.016$ ; Fig. 5G,H). We found no immunization effects in that [ $^3\text{H}$ ]PK11195-specific binding increase.

We then considered amyloid plaques as a unique entity, divided them into three groups (stage I-II, stage III-IV and immunized dogs) and analyzed the astrocytes included within 200  $\mu\text{m}$  of the plaque perimeter. In the stage III-IV plaque group, the number of S100B-IR ( $p=0.012$ ) and GFAP-IR cells ( $p=0.031$ ) and the intensity of S100B-IR ( $p<0.001$ ) were lower than the stage I-II plaques (Fig. 6C-E). The plaques from immunized dogs presented a similar number of GFAP-IR cells to stage III-IV plaques (Fig. 6C). However, they presented a lower number of associated S100B-positive astrocytes ( $p=0.050$ ), and the S100B-IR intensity in these cells was the lowest found ( $p=0.001$ ) (Fig. 6 A,B).

To gain a better understanding of the relationship between astrocytes and plaques, we subdivided the 200- $\mu\text{m}$  distance into four 50- $\mu\text{m}$  segments, and calculated the percentage of either S100B-IR or GFAP-IR present in each segment (Fig. 6F-H). In the stage I-II plaque group, the percentage of S100B-IR cells was similar in all four analyzed segments (Fig. 6F), while the furthest-away segment (150-200  $\mu\text{m}$ ) presented the highest percentage of GFAP-IR cells ( $p\chi^2=0.019$ ). In the stage III-IV plaque group, the percentage of S100B-IR cells presented a non-significant tendency to increase in

the 25-50  $\mu\text{m}$  and 50-100  $\mu\text{m}$  segments when compared to the stage I-II plaques, and the same was true of the percentage of GFAP-IR cells (Fig. 6G). In the plaques of immunized dogs this tendency to increase reached statistical significance in the percentage of GFAP-IR cells included in the 25-50  $\mu\text{m}$  and 50-100 $\mu\text{m}$  segments ( $p\chi^2=0.002$ ; Fig. 6H).

## DISCUSSION

This paper presents evidence that the anti-A $\beta$  immunotherapy developed in our laboratory [37] modifies the shape and density of A $\beta$  plaques in aged dogs, in close correlation with S100B-negative astrocytosis and microglial reaction. We also provide data that reinforce the idea that glial cell reactivity is associated with amyloid pathology and cognitive dysfunction [17,19,20]. In a previous paper, we showed that this vaccine lead to a very rapid cognitive improvement in all treated CDS dogs, with no evident side effects [37]. We also found that plasma A $\beta_{40}$  was increased but remained constant in the cerebrospinal fluid of immunized dogs. These modifications were accompanied by a 10-fold increased serum anti-A $\beta_{40}$  IgG [37]. These results established a relationship between the grade of CDS and the levels of A $\beta$  peptide in cerebrospinal fluid and plasma. We now show that immunization modifies the shape and density of A $\beta$  plaques, which argues for a modification of the equilibrium between soluble and insoluble A $\beta$  in aged dogs.

Due to the lack of reliable antibodies available to detect activated microglia in the dog brain by immunohistochemistry [46] (and personal observations), the first prominent result of this study was the description of an effective method for measuring activated microglia in the dog brain. Quantification of PBR concentration by [ $^3$ H]PK11195-specific binding to brain slices has been used extensively to estimate microglial reactivity in human and rodent brains [38,47–49]. Similarly, quantification of *in vivo* radiolabeled-PK11195 binding to the cerebral PBR is currently used to measure microglial reactivity in patients with various pathologies involving neuroinflammation, including AD patients, through modern imaging techniques [50–52]. When compared with controls, we herein found an increase in [ $^3$ H]PK11195 binding in the cerebral cortex of CDS dogs, which indicates a relationship between microglial activation and canine cognitive deterioration. This relationship, also found in human AD [53], is another of the several AD hallmarks present in the CDS dog that highlight dogs as a good model for studying

the cascade of events that take place with brain amyloid deposition, aging and dementia [12].

We previously established that S100B plays a role in the link between diffuse A $\beta$  plaque maturation and astroglial reactivity in the aging dog brain [20]. This time, we found no clear association between cognitive decline and an increase in the total number of S100B- and GFAP-positive astrocytes. This aspect may represent acute events of the animal life that have no relationship with the aging and cognitive process [18]. Including dogs with a diverse range of characteristics in the study avoided us estimating the possible influence of specific aspects like breed or sex on this result. However, our data confirm a relationship between A $\beta$  deposition and canine cognitive deficit [15,18], which may be related to alterations in brain function through common processes at the early stages of amyloid deposition, as has been suggest for AD [54,55].

We have previously designed and validated in aged dogs the efficacy and safety of a new vaccine considered a good candidate for human AD prevention and treatment [37]. When we accessed the brains of some of those immunized animals, we were able to analyze the effects of the immunization in both the inflammation and the A $\beta$  plaque shape and distribution in the brains. Our results argue for a lack microhemorrhages or inflammation associated with this immunotherapy. We describe the absence of hemosiderin-positive deposits and of CD3-immunopositive cells in the perivascular parenchyma. We also found a lack of anti-A $\beta$  antibody binding to blood vessels and a homogeneous widespread binding of [ $^3$ H]PK11195 to prefrontal cortex. These results are in line with the lack of side effects found in the clinical follow-up of this same immunized animals, and the normality of the frequent plasma and cerebrospinal fluid analyses previously published [37].

Aged dogs spontaneously develop diffuse plaques that do not fulfill the  $\beta$ -pleated sheet (equivalent to AD maturation stages I to IV) and are thioflavin negative, with no apparent neuritic component [12]. In all of the immunized dogs, we identified a new

group of smaller and more compact amyloid plaques that probably resulted from immunization. A $\beta$  immunization induces plaque clearance in both 3 $\times$ Tg-AD mice and humans (See [54] for a review). In dogs, the lack of booster doses in the immunization procedure may induce a slow course of A $\beta$  clearance that enables the plaques to be completely removed in a few months but prevents side effects. These A $\beta$  aggregates may also present differences in the biochemical composition with respect to those of non-immunized animals. In human AD, the grade of A $\beta$  phosphorylation is specifically associated with symptomatic occurrence of AD [4]. These A $\beta$  phosphorylation variations, also found in dispersible A $\beta$  oligomers, protofibrils, and fibrils, may be modified by immunization and account, at least in part, for the cognitive deficit improvement of immunized dogs.

In our previous study, we detected anti-A $\beta_{40}$  IgGs in the cerebrospinal fluid of immunized dogs [37], which demonstrates that these antibodies cross the blood-brain barrier. We herein found that these anti-A $\beta_{40}$  IgGs recognize diffuse non-fibrillar plaques much more easily than neuritic ones or blood vessels. Thus, antibodies may recognize diffuse plaques and activate a neuroinflammatory response that would lead to smaller and more compact amyloid plaques with consequences for the soluble-insoluble A $\beta$  equilibrium between the brain and blood [37]. If this is true, immunized dogs should present changes in neuroinflammatory activity when compared with control animals.

In the aged dogs, we found hypertrophic astrocytes overexpressing GFAP and S100B generally located just outside the plaque boundary. This distribution is associated with plaque stage and proximity and is related to cognitive status [20], as has also been described for AD [7,56,57]. In the brains of the immunized aged dogs, we found a lower number of reactive astrocytes related to A $\beta$  plaques. These astrocytes were less immunoreactive to S100B and GFAP and were grouped more closely to the plaques. Activated S100B-IR astrocytes are related to the induction and maintenance of dystrophic neurites in amyloid plaques [24,58], due to amyloid toxicity. For that reason,

S100B has been considered an important pathogenic factor in the genesis and evolution of plaques in AD. The reduced S100B-IR of astrocytes may therefore lead to the recovery of dystrophic neurites and the subsequent reduction in amyloid plaque processes. Thus, the decrease in S100B overexpression appears in the plaques of immunized dogs; these plaques correspond to the more compact stage of plaque maturation and present a shorter astrocyte–plaque distance. We previously described a correlation between canine graded cognitive deficit, diffuse plaque maturation, and S100B-astrocytosis [20]. Thus, astroglial reactivity around the plaque varies according to plaque maturation, and S100B positive astrocytes are involved in the more advanced stages of maturation and cognitive deficit. Based on that, the reduced intensity of S100B-IR, but not GFAP-IR, in astrocytes close to plaques of immunized dogs we herein found, may be related with the improved cognitive deficit of these immunized CDS animals [37]. Also, the correlation between S100B overexpression and the more significant impairments argues for astrocyte participation in autocrine and paracrine effects associated with the neurodegenerative process [20,23]. To approach this putative relationship, further experiments are needed with a higher number of immunized CDS dogs.

At physiological levels, S100B exerts a protective effect, but when it increases, its interactions with other cytokines and microglial cells potentiate the activation of microglial, neurodegenerative or apoptosis-inducing effects. Therefore, the absence of a microglial reaction specifically associated with diffuse plaques in our study may be related to lower plaque–astrocyte interactions and reactivity. Together with the absence of microglial cells in AD diffuse plaques [58], our data suggest that the involvement of S100B and microglia in the progression of AD does not initiate in the very early stages of plaque formation. However, we found an increase in the homogeneous widespread binding of [<sup>3</sup>H]PK11195 in the cerebral cortex of CDS dogs, which would suggest that microglia are involved in the initiation and maintenance of amyloid pathology [50]. Microglial activity in AD is a controversial subject. While

numerous studies in animal models of AD have demonstrated that modulating microglial activation can be a powerful strategy for clearing A $\beta$  plaques, it is also thought that A $\beta$  might not adequately activate microglia effector functions to clear the accumulating amyloid burden from the brain [53]. Our results showed that A $\beta$  immunization does not modify the distribution and increase of [ $^3$ H]PK11195 in CDS dogs. However, other changes in microglial activity may occur. As explained for AD [60], A $\beta$  immunization specifically increases the phagocytic activity of microglia, which would contribute to fibrillar-soluble A $\beta$  clearance and lead to plaque compaction and decreased amyloid toxicity. Taken together, all these neuroinflammatory changes may contribute, at least in part, to the cognitive improvement of immunized CDS dogs observed after several weeks of treatment.

In conclusion, in this study we demonstrated that the anti-A $\beta$  immunotherapy developed in our laboratory modifies the shape and density of plaques in aged dogs in close correlation with S100B-negative astrocytosis and microglial reaction. Together with our previous study in which we described a cognitive improvement and a shift in equilibrium between soluble and insoluble A $\beta$  in immunized dogs, our overall results indicate that immunotherapy decreases A $\beta$  toxicity and reaffirm the interest of the anti-A $\beta$  immunotherapy as a possible treatment for the canine CDS and human AD. Future studies would be necessary for a better characterization of the immunization effects on A $\beta$  biochemical composition and the interplay between the S100B-positive astrocytes, microglia and A $\beta$  burden.

## ACKNOWLEDGEMENTS

We thank Medivet Pharma SL (Masies de Roda, Barcelona, Spain) and the Ars Veterinaria Hospital (Barcelona, Spain) for their help in brain sample collection and the dog clinical assessment respectively.

## DISCLOSURE

MP, NM and MJR hold an EU patent (No. WO2010/012749) exploited by Medivet Pharma, SL and hold shares of the company. The other authors report no disclosures.

## REFERENCES

- 1 Crews L, Masliah E. Molecular mechanisms of neurodegeneration in Alzheimer's disease. *Hum Mol Genet* 2010; 19:R12–20.
- 2 Ballard C, Gauthier S, Corbett A, *et al.* Alzheimer's disease. *Lancet* 2011; 377:1019–3101.
- 3 Hardy J, Selkoe DJ. The Amyloid Hypothesis of Alzheimer's Disease: Progress and Problems on the Road to Therapeutics. *Science* 2002; 297:353–356.
- 4 Rijal Upadhaya A, Kosterin I, Kumar S, *et al.* Biochemical stages of amyloid- $\beta$  peptide aggregation and accumulation in the human brain and their association with symptomatic and pathologically preclinical Alzheimer's disease. *Brain* 2014; 137:887-903.
- 5 Karran E, Mercken M, De Strooper B. The amyloid cascade hypothesis for Alzheimer's disease: an appraisal for the development of therapeutics. *Nat Rev Drug Discov* 2011; 10:698–712.
- 6 D'Andrea MR, Cole GM, Ard MD. The microglial phagocytic role with specific plaque types in the Alzheimer disease brain. *Neurobiol Aging* 2004; 25:675–683.
- 7 De Witt DA, Perry G, Cohen M, *et al.* Astrocytes Regulate Microglial Phagocytosis of Senile Plaque Cores of Alzheimer's Disease. *Exp Neurol* 1998; 149:329–40.
- 8 Morgan D, Gordon MN, Tan J, *et al.* Dynamic complexity of the microglial activation response in transgenic models of amyloid deposition: implications for Alzheimer therapeutics. *J Neuropathol Exp Neurol* 2005; 64:743–753.
- 9 Ruehl WW, Bruyette DS, DePaoli A, *et al.* Canine cognitive dysfunction as a model for human age-related cognitive decline, dementia and Alzheimer's disease: clinical presentation, cognitive testing, pathology and response to 1-deprenyl therapy. *Prog Brain Res* 1995; 106:217–225.
- 10 Pugliese M, Carrasco JL, Andrade C, *et al.* Severe cognitive impairment correlates with higher cerebrospinal fluid levels of lactate and pyruvate in a canine model of senile dementia. *Prog Neuropsychopharmacol Biol Psychiatry* 2005; 29:603–610.
- 11 Rofina JE, van Ederen AM, Toussaint MJM, *et al.* Cognitive disturbances in old dogs suffering from the canine counterpart of Alzheimer's disease. *Brain Res* 2006; 1069:216–226.
- 12 Bosch MN, Pugliese M, Gimeno-Bayón J, *et al.* Dogs with cognitive dysfunction syndrome: a natural model of Alzheimer's disease. *Curr Alzheimer Res* 2012; 9:298–314.
- 13 Cotman CW, Head E. The Canine (Dog) Model of Human Aging and Disease: Dietary, Environmental and Immunotherapy Approaches. *J Alzheimers Dis* 2008;15: 685–707.
- 14 Vasilevko V, Head E. Immunotherapy in a natural model of Abeta pathogenesis: the aging beagle. *CNS Neurol Disord Drug Targets* 2009; 8:98–113.

- 15 Cummings BJ, Head E, Afagh AJ, *et al.* [beta]-Amyloid Accumulation Correlates with Cognitive Dysfunction in the Aged Canine. *Neurobiol Learn Mem* 1996; 66:11–23. 9
- 16 Hou Y, White RG, Bobik M, *et al.* Distribution of beta-amyloid in the canine brain. *Neuroreport* 1997; 8:1009–1012.
- 17 Papaioannou N, Tooten PC, van Ederen AM, *et al.* Immunohistochemical investigation of the brain of aged dogs. I. Detection of neurofibrillary tangles and of 4-hydroxynonenal protein, an oxidative damage product, in senile plaques. *Amyloid Int J Exp Clin Investig* 2001;8:11–21.
- 18 Pugliese M, Mascort J, Mahy N, *et al.* Diffuse beta-amyloid plaques and hyperphosphorylated tau are unrelated processes in aged dogs with behavioral deficits. *Acta Neuropathol (Berl)* 2006; 112:175–183.
- 19 Shimada A, Kuwamura M, Awakura T, *et al.* An immunohistochemical and ultrastructural study on age-related astrocytic gliosis in the central nervous system of dogs. *J Vet Med Sci* 1992; 54:29–36.
- 20 Pugliese M, Geloso MC, Carrasco JL, *et al.* Canine cognitive deficit correlates with diffuse plaque maturation and S100 $\beta$  (-) astrocytosis but not with insulin cerebrospinal fluid level. *Acta Neuropathol (Berl)* 2006; 111:519–528.
- 21 Sheng JG, Mrak RE, Griffin WS. Neuritic plaque evolution in Alzheimer's disease is accompanied by transition of activated microglia from primed to enlarged to phagocytic forms. *Acta Neuropathol (Berl)* 1997; 94:1–5.
- 22 Mackenzie IR, Hao C, Munoz DG. Role of microglia in senile plaque formation. *Neurobiol Aging* 1995; 16:797–804.
- 23 Adami C, Sorci G, Blasi E, *et al.* S100b expression in and effects on microglia. *Glia* 2001; 33:131–142.
- 24 Mrak RE, Griffin WS. The role of activated astrocytes and of the neurotrophic cytokine S100B in the pathogenesis of Alzheimer's disease. *Neurobiol Aging* 2001; 22:915–922.
- 25 Kilby PM, Van Eldik LJ, Roberts GC. Identification of the binding site on S100B protein for the actin capping protein CapZ. *Protein Sci* 1997; 6:2494–2503.
- 26 Demattos RB, Lu J, Tang Y, *et al.* A plaque-specific antibody clears existing  $\beta$ -amyloid plaques in Alzheimer's disease mice. *Neuron* 2012; 76:908–920.
- 27 Zhang Y, He J-S, Wang X, *et al.* Administration of amyloid- $\beta$ 42 oligomer-specific monoclonal antibody improved memory performance in SAMP8 mice. *J Alzheimers Dis* 2011;23:551–561.
- 28 Bohrmann B, Baumann K, Benz J, *et al.* Gantenerumab: a novel human anti-A $\beta$  antibody demonstrates sustained cerebral amyloid- $\beta$  binding and elicits cell-mediated removal of human amyloid- $\beta$ . *J Alzheimers Dis* 2012; 28:49–69.
- 29 Kingwell K. Alzheimer disease: Amyloid- $\beta$  immunotherapy CAD106 passes first safety test in patients with Alzheimer disease. *Nat Rev Neurol* 2012; 8:414.

- 30 Lemere CA, Masliah E. Can Alzheimer disease be prevented by amyloid-[beta] immunotherapy? *Nat Rev Neurol* 2010; 6:108–119.
- 31 Panza F, Frisardi V, Imbimbo BP, *et al.* Bapineuzumab: anti- $\beta$ -amyloid monoclonal antibodies for the treatment of Alzheimer's disease. *Immunotherapy* 2010; 2:767–82.
- 32 Wiessner C, Wiederhold K-H, Tissot AC, *et al.* The second-generation active A $\beta$  immunotherapy CAD106 reduces amyloid accumulation in APP transgenic mice while minimizing potential side effects. *J Neurosci* 2011;31:9323–9331.
- 33 Gilman S, Koller M, Black RS, *et al.* Clinical effects of A{beta} immunization (AN1792) in patients with AD in an interrupted trial. *Neurology* 2005; 64:1553–1562.
- 34 Orgogozo J-M, Gilman S, Dartigues J-F, *et al.* Subacute meningoencephalitis in a subset of patients with AD after Abeta42 immunization. *Neurology* 2003; 61:46–54.
- 35 Liu Y-H, Giunta B, Zhou H-D, *et al.* Immunotherapy for Alzheimer disease: the challenge of adverse effects. *Nat Rev Neurol* 2012; 8:465–469.
- 36 Menéndez-González M, Pérez-Piñera P, Martínez-Rivera M, *et al.* Immunotherapy for Alzheimer's disease: rational basis in ongoing clinical trials. *Curr Pharm Des* 2011; 17:508–520.
- 37 Bosch MN, Gimeno-Bayón J, Rodríguez MJ, *et al.* Rapid improvement of canine cognitive dysfunction with immunotherapy designed for Alzheimer's disease. *Curr Alzheimer Res* 2013; 105:482-493.
- 38 Bernal F, Petegnief V, Rodríguez MJ, *et al.* Nimodipine inhibits TMB-8 potentiation of AMPA-induced hippocampal neurodegeneration. *J Neurosci Res* 2009; 87:1240–129.
- 39 Rodríguez MJ, Martínez-Sánchez M, Bernal F, *et al.* Heterogeneity between hippocampal and septal astroglia as a contributing factor to differential in vivo AMPA excitotoxicity. *J Neurosci Res* 2004; 77:344–353. doi:10.1002/jnr.20177
- 40 Saura J, Nadal E, van den Berg B, *et al.* Localization of monoamine oxidases in human peripheral tissues. *Life Sci* 1996; 59:1341–1349.
- 41 De Yebra L, Malpesa Y, Ursu G, *et al.* Dissociation between hippocampal neuronal loss, astroglial and microglial reactivity after pharmacologically induced reverse glutamate transport. *Neurochem Int* 2006; 49:691–697.
- 42 Mahy N. Brain banks and research in neurochemistry. *J Neural Transm Suppl* 1993; 39:119–126.
- 43 Braak H, Braak E. Demonstration of amyloid deposits and neurofibrillary changes in whole brain sections. *Brain Pathol Zurich Switz* 1991; 1:213–216.
- 44 Luo F, Rustay NR, Seifert T, *et al.* Magnetic resonance imaging detection and time course of cerebral microhemorrhages during passive immunotherapy in living amyloid precursor protein transgenic mice. *J Pharmacol Exp Ther* 2010; 335:580-588.

- 45 Braak H, Braak E. Neuropathological staging of Alzheimer-related changes. *Acta Neuropathol (Berl)* 1991; 82:239–259.
- 46 Stein VM, Baumgärtner W, Kreienbrock L, *et al.* Canine microglial cells: stereotypy in immunophenotype and specificity in function? *Vet Immunol Immunopathol* 2006; 113:277–287.
- 47 Miller TR, Wetter JB, Jarvis MF, *et al.* Spinal microglial activation in rat models of neuropathic and osteoarthritic pain: an autoradiographic study using [3H]PK11195. *Eur J Pain Lond Engl* 2013; 17:692–703.
- 48 Stephenson DT, Schober DA, Smalstig EB, *et al.* Peripheral benzodiazepine receptors are colocalized with activated microglia following transient global forebrain ischemia in the rat. *J Neurosci Off J Soc Neurosci* 1995; 15:5263–5274.
- 49 Vowinckel E, Reutens D, Becher B, *et al.* PK11195 binding to the peripheral benzodiazepine receptor as a marker of microglia activation in multiple sclerosis and experimental autoimmune encephalomyelitis. *J Neurosci Res* 1997; 50:345–353.
- 50 Edison P, Archer HA, Gerhard A, *et al.* Microglia, amyloid, and cognition in Alzheimer's disease: An [11C](R)PK11195-PET and [11C]PIB-PET study. *Neurobiol Dis* 2008; 32:412–419. doi:10.1016/j.nbd.2008.08.001
- 51 Kumar A, Muzik O, Shandal V, *et al.* Evaluation of age-related changes in translocator protein (TSPO) in human brain using (11)C-[R]-PK11195 PET. *J Neuroinflammation* 2012; 9:232.
- 52 Venneti S, Lopresti BJ, Wang G, *et al.* PK11195 labels activated microglia in Alzheimer's disease and in vivo in a mouse model using PET. *Neurobiol Aging* 2009;30:1217–1226.
- 53 Prokop S, Miller KR, Heppner FL. Microglia actions in Alzheimer's disease. *Acta Neuropathol (Berl)* 2013; 126:461–477.
- 54 McGeer PL, McGeer EG. The amyloid cascade-inflammatory hypothesis of Alzheimer disease: implications for therapy. *Acta Neuropathol (Berl)* 2013; 126:479–497.
- 55 Morris JC, Storandt M, McKeel DW Jr, *et al.* Cerebral amyloid deposition and diffuse plaques in 'normal' aging: Evidence for presymptomatic and very mild Alzheimer's disease. *Neurology* 1996; 46:707–719.
- 56 Medeiros R, Laferla FM. Astrocytes: Conductors of the Alzheimer disease neuroinflammatory symphony. *Exp Neurol* 2013; 239:133–138.
- 57 Nagele RG, Wegiel J, Venkataraman V, *et al.* Contribution of glial cells to the development of amyloid plaques in Alzheimer's disease. *Neurobiol Aging* 2004; 25:663–674.
- 58 Mrak RE, Sheng JG, Griffin WS. Correlation of astrocytic S100 beta expression with dystrophic neurites in amyloid plaques of Alzheimer's disease. *J Neuropathol Exp Neurol* 1996; 55:273–279.
- 59 Ohgami T, Kitamoto T, Shin RW, *et al.* Increased senile plaques without microglia in Alzheimer's disease. *Acta Neuropathol (Berl)* 1991; 81:242–247.

- 60 Zotova E, Holmes C, Johnston D, *et al.* Microglial alterations in human Alzheimer's disease following A $\beta$ 42 immunization. *Neuropathol Appl Neurobiol* 2011; 37:513–524.

## FIGURE LEGENDS

**Fig. 1:** *Immunization procedure.* Five dogs received six injections of a fibrillar A $\beta$  vaccine over a period of 51 days. Serum from all immunized dogs was collected on day 51 of the follow-up. Each animal was sacrificed after a different period of time (Table 1)

**Fig. 2:** *Comparison of glial reactivity between non-demented and CDS dogs.* The number of immunoreactive S100B and GFAP astrocytes (A-C), intensity of S100B-IR in the cytoplasm (B) and concentration of specific [ $^3$ H]PK11195 binding to the PBR (D) were measured and compared between non-demented (control) and CDS dogs. We observed higher levels of specific [ $^3$ H]PK11195 binding to the PBR in CDS than in control dogs, indicating more activated microglia in these dogs (\*, p=0.034). When immunized dogs were included in the comparison, only a non-significant tendency for the intensity of cytoplasmatic S100B-IR to decrease was observed.

**Fig. 3:** *Detection of human amyloid plaques with purified anti-A $\beta$  IgGs from immunized dogs.* Immunohistochemistry using commercial anti-A $\beta$  IgGs or purified anti-A $\beta$  IgGs as a primary antibody were performed in samples from AD patients in stage II and stage VI of the Braak & Braak scale. (A, C) Commercial antibodies can detect neuritic plaques (black arrows) and leptomenigeal blood vessels (arrowheads) in AD stage VI samples more effectively. However, (B, D) purified antibodies can detect diffuse plaques (black arrows) more effectively, but not leptomenigeal blood vessels (arrowheads). Panels E, F show double immunohistochemistry to detect anti-A $\beta$  IgGs (red) and ThT+ (blue) and show that fibrillar amyloid plaques were not detected by purified anti-A $\beta$  IgGs, while anti-A $\beta$  labeling with commercial antibodies shows them as co-localized with ThT+ plaques (pink). Scale bars: 200  $\mu$ m (A – D); 50  $\mu$ m (inset in C, D and E, F).

**Fig. 4:** *Histological study of brain microhemorrhages or lymphocyte infiltration induced by immunization.* (A-C) Perl's Prussian blue counterstained with neutral red identified hemosiderin deposits in dog liver slices (arrows in A) but not in the perivascular prefrontal cortex of immunized control (B) and CDS (C) dogs. (D-F) Immunohistochemistry with specific anti-CD3 antibodies stained in dark brown lymphocytes in dog spleen slices (D) but not in the prefrontal cortex of immunized control (E) and CDS (F) dogs. Asterisks identify blood vessels. Scale bar, 50  $\mu\text{m}$

**Fig. 5:** *Amyloid plaque detection, classification and relationship with glial reactivity.* (A-C) Study of plaque size and density. Illustrative photomicrographs of amyloid plaques from the prefrontal cortex (A), which were classified in: 1) Stages I-II, with large, slightly compacted plaques situated in the deeper layers of the prefrontal cortex. 2) Stages III-IV, with smaller and more compacted plaques situated in layers II-III or throughout all layers of the prefrontal cortex. 3) Plaques from immunized dogs, with the smallest and most compacted shape. Plaques from immunized dogs were significantly smaller (B) and presented increased labeling (C) than stage I-II plaques (\*,  $p=0.036$  for the size and  $p=0.033$  for the  $\text{A}\beta$  labeling). (D-G) In accordance with the above classification, histograms show quantification of (D) the number of S100B-IR cells, (E) the intensity of S100B cytoplasmic staining (\*,  $p=0.016$  vs no plaques), (F) the number of GFAP-IR cells, and (G) [ $^3\text{H}$ ]PK11195-specific binding (\* $p=0.015$  vs no plaques). (H) Illustrative photomicrographs of the distribution of specific binding sites for [ $^3\text{H}$ ]PK11195 in dog brain sections with no amyloid plaques and with stage III-IV plaques. Scale bar, 100  $\mu\text{m}$  (A), and 3 mm (H)

**Fig. 6:** *Immunoreactive GFAP and S100B astrocytes associated with the amyloid plaque.* Illustrative photomicrographs of either GFAP-IR or S100B-IR cells in brain sections of dogs presenting stage I-II plaques (A) and immunized dogs (B). Quantification of the GFAP-IR and S100B-IR cells within 200  $\mu\text{m}$  of the plaque.

Histograms show (C) the number of S100B-IR cells, (&,  $p=0.012$ ; #,  $p=0.050$ ), (D) the intensity of S100B cytoplasmic staining (\*\*,  $p<0.001$ , #,  $p=0.001$ ) and (E) number of GFAP-IR cells astrocytes (\*,  $p=0.031$ ). To estimate the differences in the astrocyte-plaque association, we then divided the distance of 200  $\mu\text{m}$  into four 50- $\mu\text{m}$  segments and calculated the percentage of both GFAP-IR and S100B-IR cells (arrows in pictures) located in each segment (F-H). GFAP-IR cells associated with plaques from immunized dogs (H) showed a non-significant tendency to be located in the closest segments when compared to stage I-II (F) and stage III-IV (G) plaques. This tendency was not observed for S100B-IR cells. ( $p\chi^2=0.019$  for 150-200  $\mu\text{m}$  in stage I-II;  $p\chi^2=0.002$  for 25-50  $\mu\text{m}$ , 50-100  $\mu\text{m}$  in plaques from immunized dogs) (5 amyloid plaques / sample).

Table 1: Dogs included in the study.

ID	Breed	Age	Cognitive Group	Immunization group	LTI (weeks)	Plaque stage	A $\beta$ / glia IHQ
1	Beagle	3	Non Demented	Unimmunized		0	
2	Cocker	1	Non Demented	Unimmunized		0	
3	Poodle	6	Non Demented	Unimmunized		0	
4	Mixed	1	Non Demented	Unimmunized		0	
5	Mixed	7	Non Demented	Unimmunized		0	
6	Yorkshire	8	Non Demented	Unimmunized		0	
7	Schnauzer	8	Non Demented	Unimmunized		I-II	+
8	Poodle	15	Non Demented	Unimmunized		I-II	+
9	German Shepherd	10	CDS	Unimmunized		I-II	+
10	Poodle	11	CDS	Unimmunized		I-II	
11	Mixed	13	CDS	Unimmunized		III-IV	+
12	Boxer	15	CDS	Unimmunized		I-II	+
13	Mixed	14	CDS	Unimmunized		0	
14	Poodle	14	CDS	Unimmunized		I-II	+
15	Pekingese	15	CDS	Unimmunized		III-IV	+
16	Mixed	16	CDS	Unimmunized		III-IV	+
17	Fox Terrier	16	CDS	Unimmunized		III-IV	
18	Mixed	20	CDS	Unimmunized		III-IV	+
19	Beagle	6	Non Demented	Immunized	41	0	
20	Beagle	8	Non Demented	Immunized	31	0	
21	Mixed	12	Non Demented	Immunized	40	Immunized	+
22	Mixed	13	Non Demented	Immunized	32	Immunized	+
23	Mixed	15	CDS	Immunized	38	Immunized	+

CDS, cognitive dysfunction syndrome; LTI, live time after immunization; IHQ, immunohistochemistry

Figure 1

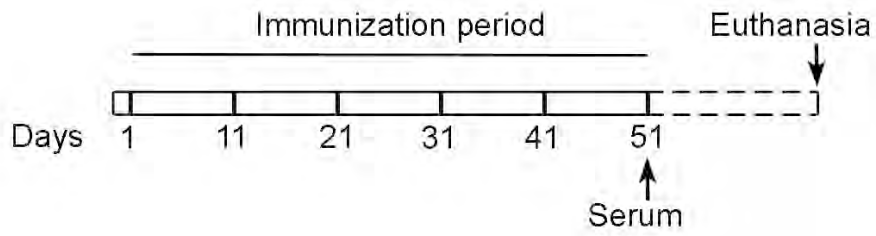


Figure 2

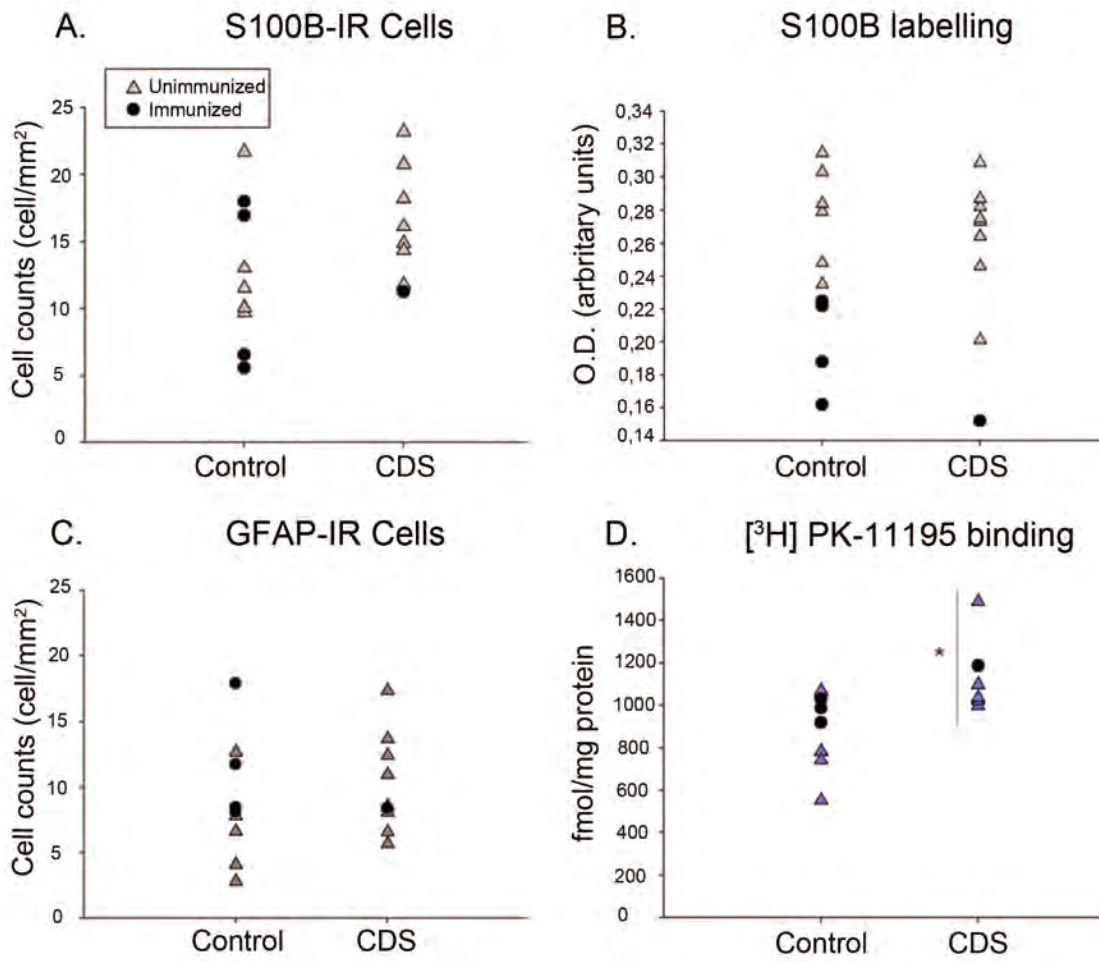


Figure 3

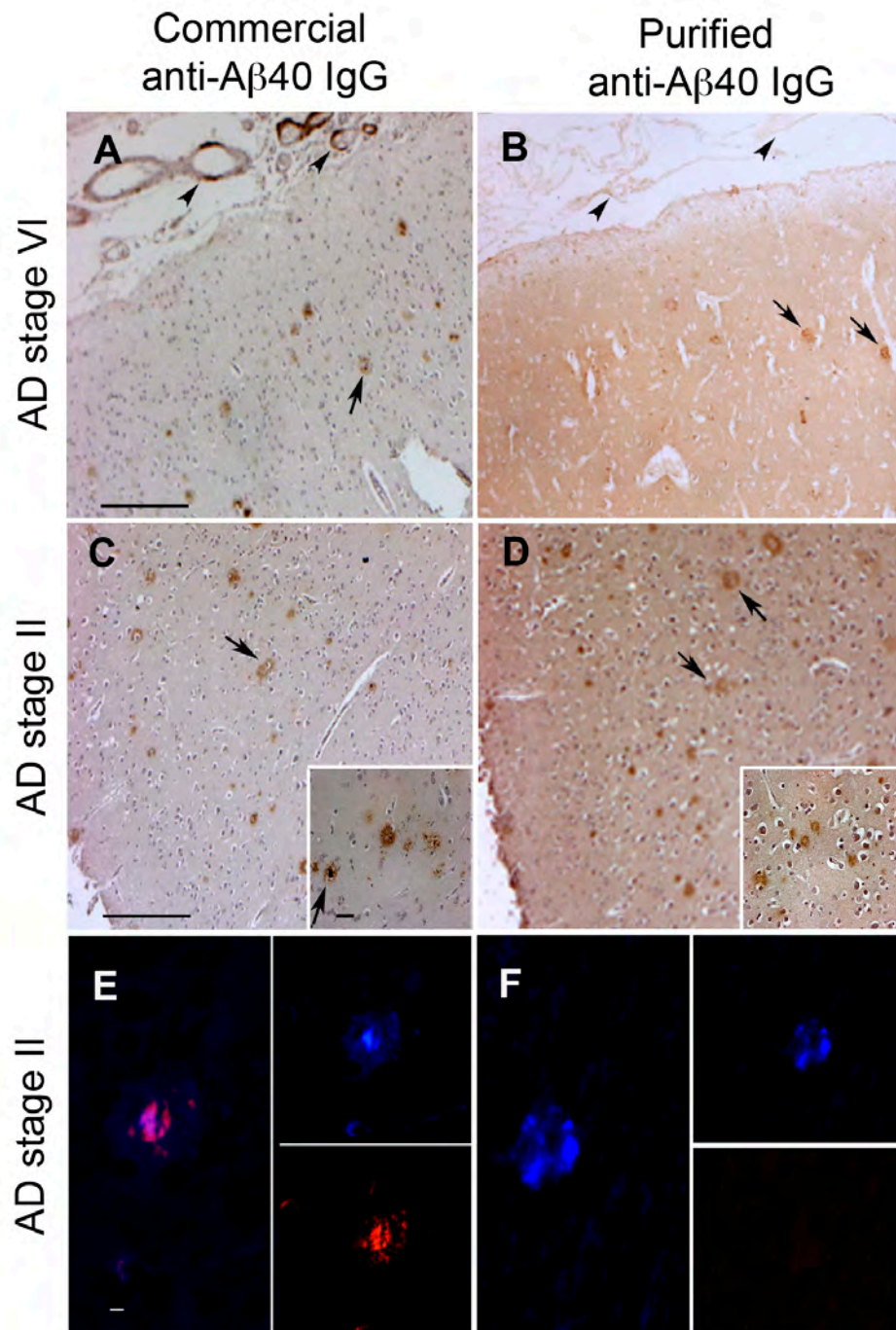


Figure 4

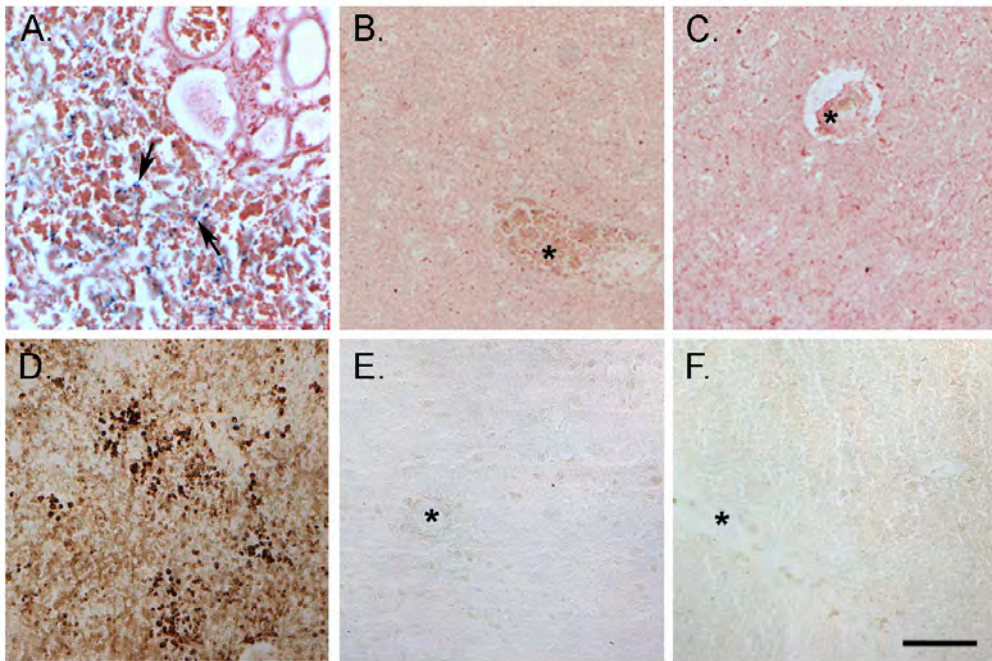
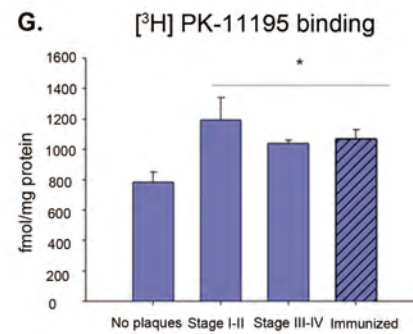
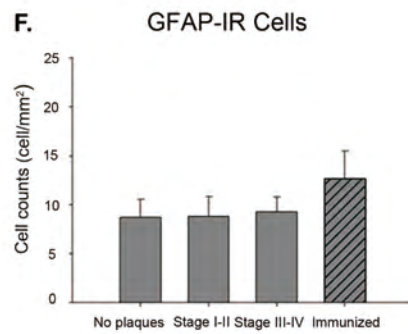
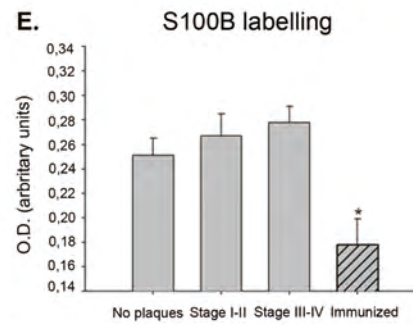
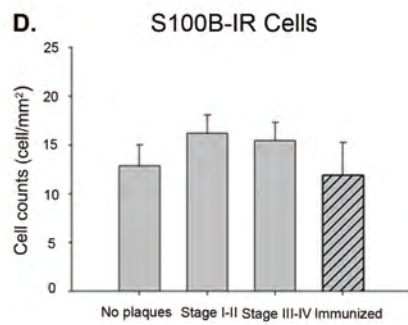
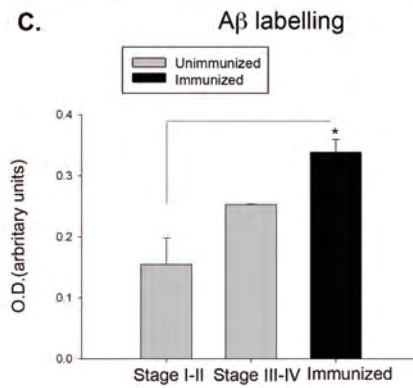
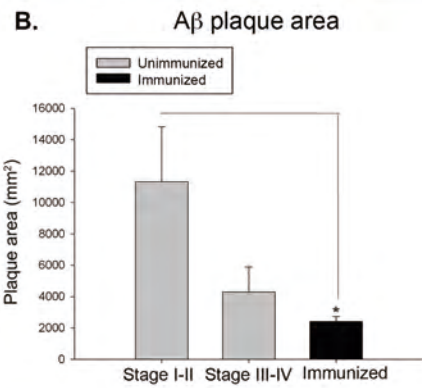


Figure 5



**H. [<sup>3</sup>H] PK-11195 binding to frontal cortex of dogs**

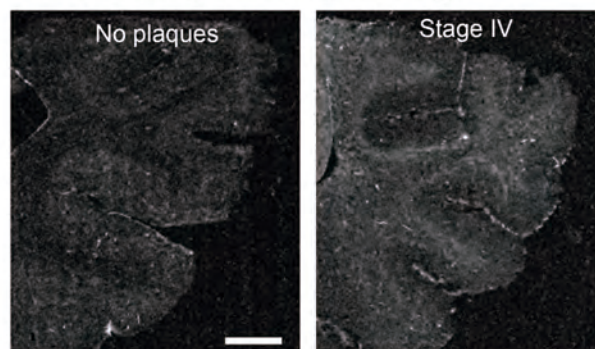


Figure 6

